Cell Stem Cell
Article

Reactive Glia in the Injured Brain Acquire Stem Cell Properties in Response to Sonic Hedgehog

Swetlana Sirko,[1,4,14] Gwendolyn Behrendt,[1,14] Pia Annette Johansson,[4] Pratibha Tripathi,[4,15] Marcos Romualdo Costa,[4,16] Sarah Bek,[1,4] Christophe Heinrich,[1] Steffen Tiedt,[1] Dilek Colak,[4,5] Martin Dichgans,[6,7] Isabel Rebekka Fischer,[6] Nikolaus Plesnila,[6,7] Matthias Staufenbiel,[8] Christian Haass,[2,3,7] Marina Snapyan,[9] Armen Saghatelyan,[9] Li-Huei Tsai,[10,11] André Fischer,[12] Kay Grobe,[13] Leda Dimou,[1,4] and Magdalena Götz[1,4,7,*]

[1]Physiological Genomics, Institute of Physiology
[2]German Center for Neurodegenerative Diseases (DZNE)
[3]Adolf-Butenandt-Institute, Biochemistry
Ludwig-Maximilians University Munich, D-80336, Germany
[4]Institute for Stem Cell Research, Helmholtz Zentrum Munich, German Research Center for Environmental Health, Neuherberg/Munich, D-85764, Germany
[5]Department of Pharmacology, Weill Medical College of Cornell University, New York, NY 10021, USA
[6]Institute for Stroke and Dementia Research, Ludwig-Maximilians University Munich, D-81377, Germany
[7]Munich Cluster for Systems Neurology (SyNergy), Munich D-80336, Germany
[8]Department of Neuroscience Institutes for BioMedical Research, Novartis Pharma AG, CH-4057 Basel, Switzerland
[9]Cellular Neurobiology Unit, Institut Universitaire en Santé Mentale de Québec, Université Laval, Quebec City, QC, G1J 2G3, Canada
[10]Department of Brain and Cognitive Sciences, Picower Institute for Learning and Memory, Massachusetts Institute of Technology, Cambridge, MA 02139-4307, USA
[11]Howard Hughes Medical Institute
[12]Department of Psychiatry and Psychotherapy, University Medical Center & German Center for Neurodegenerative Diseases (DZNE), Göttingen, D-37077, Germany
[13]Institute for Physiological Chemistry and Pathobiochemistry, Westfälische Wilhelms University Münster, D-48149, Germany
[14]These authors contributed equally to this work
[15]Present address: Department of Stem Cell and Regenerative Biology, Harvard University, Cambridge, MA 02138, USA
[16]Present address: Brain Institute, Federal University of Rio Grande do Norte, Natal, 59056-450, Brazil
*Correspondence: magdalena.goetz@helmholtz-muenchen.de
http://dx.doi.org/10.1016/j.stem.2013.01.019

SUMMARY

As a result of brain injury, astrocytes become activated and start to proliferate in the vicinity of the injury site. Recently, we had demonstrated that these reactive astrocytes, or glia, can form self-renewing and multipotent neurospheres in vitro. In the present study, we demonstrate that it is only invasive injury, such as stab wounding or cerebral ischemia, and not noninvasive injury conditions, such as chronic amyloidosis or induced neuronal death, that can elicit this increase in plasticity. Furthermore, we find that Sonic hedgehog (SHH) is the signal that acts directly on the astrocytes and is necessary and sufficient to elicit the stem cell response both in vitro and in vivo. These findings provide a molecular basis for how cells with neural stem cell lineage emerge at sites of brain injury and imply that the high levels of SHH known to enter the brain from extraneural sources after invasive injury can trigger this response.

INTRODUCTION

Reactive gliosis is the prototypical response of the central nervous system (CNS) to diverse types of injury mediated by various cell types and involves the activation of microglia and all classes of macroglia: oligodendrocytes, NG2+ glia, and astroglia (Göritz et al., 2011; Robel et al., 2011a; Sofroniew, 2009). Recently, cells reacting to injury have been observed to reactivate stem cell potential (Robel et al., 2011a), but the signals eliciting this response remain undefined. After traumatic brain injury, a significant fraction of the cells isolated from injured CNS tissue has been shown to generate multipotent, self-renewing cells in vitro (Barnabé-Heider et al., 2010; Buffo et al., 2008; Lang et al., 2004; Sirko et al., 2009). Genetic fate mapping identified a subtype of reactive astrocytes in the forebrain gray matter (GM) as the source of the cells that exhibit such neural stem cell (NSC) properties in vitro (Buffo et al., 2008), while in the spinal cord ependymal cells display these hallmarks (Barnabé-Heider et al., 2010).

Cells that can take on an NSC character after injury could provide an important new resource for endogenous repair and could be particularly valuable in the case of neurodegenerative diseases associated with widespread neuronal damage, such as Alzheimer's disease (AD) (Duyckaerts et al., 2009; Rodríguez et al., 2009). This prompts the question of the extent to which chronic neurodegeneration may actually elicit an NSC response. We addressed this question by comparing responses to acute ischemic lesion, traumatic injury, progressive (chronic) amyloid plaque deposition, and a noninvasive model of widespread neuronal death. To study the effects of progressive plaque deposition, we took advantage of APPPS1 mice. This mouse strain

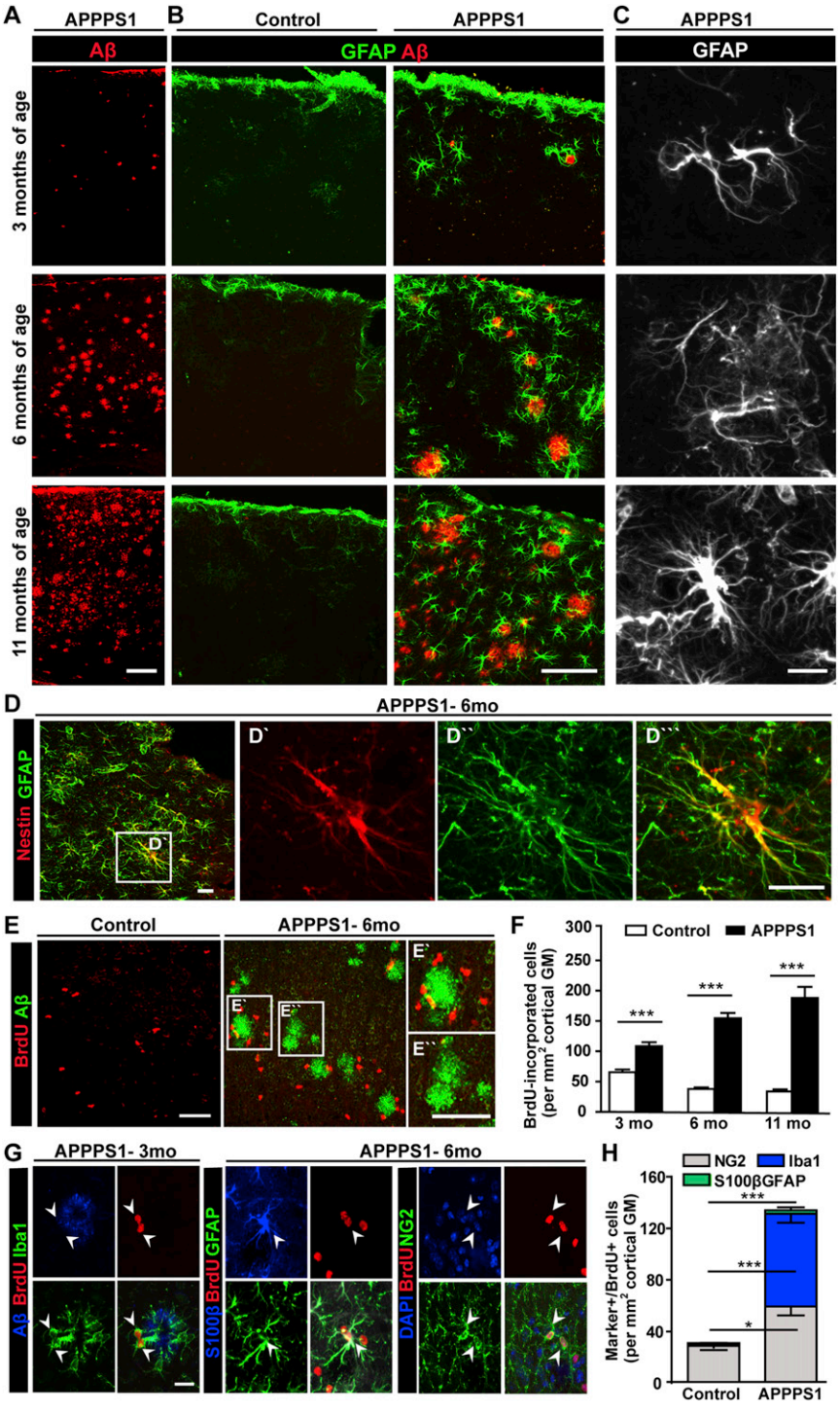

Figure 1. Reactive Gliosis and Proliferation in the Cerebral Cortex of APPPS1 Mice

(A) Representative micrographs of Aβ plaques detected by the monoclonal antibody (mAb) 6E10 in the cerebral cortex of APPPS1 mice at 3, 6, and 11 months of age. High-power views of sections stained with 6E10 and anti-GFAP are shown in (B). (C) Examples of hypertrophic astrocytes in APPPS1 mice at the ages indicated. (D) Distribution of GFAP- and nestin-expressing cells in the cerebral cortex of 6-month-old APPPS1 mice, and high-power views of separate (D′ and D″) and merged (D‴) signals. (E–H) Proliferation activity (BrdU-labeled cells) and immunohistochemical characterization of cell types in the cerebral cortex of APPPS1 mice of the indicated age. The data are quantified in the histograms shown in (F) and (H) as mean number (±SEM) per area in a section analyzed from 3–11 animals. Significant differences relative to controls are indicated by asterisks based on the p value. For additional analysis of the cerebral cortex of APPPS1 mice, see Figure S1. Scale bars: (A) and (B), 100 μm; (C) and (E), 50 μm; (D) and (G); 20 μm.

carries the Swedish double mutation, which results in overexpression of mutant forms of both the amyloid precursor protein (APP) and presenilin 1 (PS1) in neurons (Radde et al., 2006; Rupp et al., 2011). The consequences of endogenously induced neuronal death on reactive glia were examined after targeted activation of p25 expression in neurons of the cerebral cortex. This activator of cyclin-dependent kinase 5 (CDK5) elicits extensive loss of neurons, tau pathology, and intraneuronal Aβ accumulation, thus mimicking further hallmarks of AD (Cruz et al., 2003, 2006). Analysis of these acute and chronic models revealed striking differences in the proliferative response of reactive glia and the appearance of cells with NSC properties, which enabled us to identify Sonic hedgehog (SHH) as a key regulator of the stem cell response in reactive glia.

RESULTS

Reactive Astrocytes Show Low Proliferative Activity in APPPS1 Mice

To examine the glial reaction over time in the presence of continuing amyloid plaque deposition, we first used immunostaining for Aβ to visualize amyloid plaques at 3 months of age in the brains of APPPS1 mice (Radde et al., 2006) and their subsequent spread throughout the cerebral cortex within the next months (Figure 1A). Hypertrophic astrocytes that were immunoreactive for glial fibrillary acidic protein (GFAP) were mostly located in the vicinity of plaques in 3-month-old APPPS1 (APPPS1-3mo) mice and were detected in all neuronal layers at later times (Figures 1B and 1C). Many reactive astrocytes located in the GM of the cerebral cortex were also found to express proteins characteristic of immature glia or NSCs, such as nestin (Figure 1D), the membrane-associated proteoglycan DSD1 (the 473HD epitope), and tenascin-C (TNC, Figures S1A and S1B available online), all of which are typically upregulated in reactive astrocytes (Robel et al., 2011a).

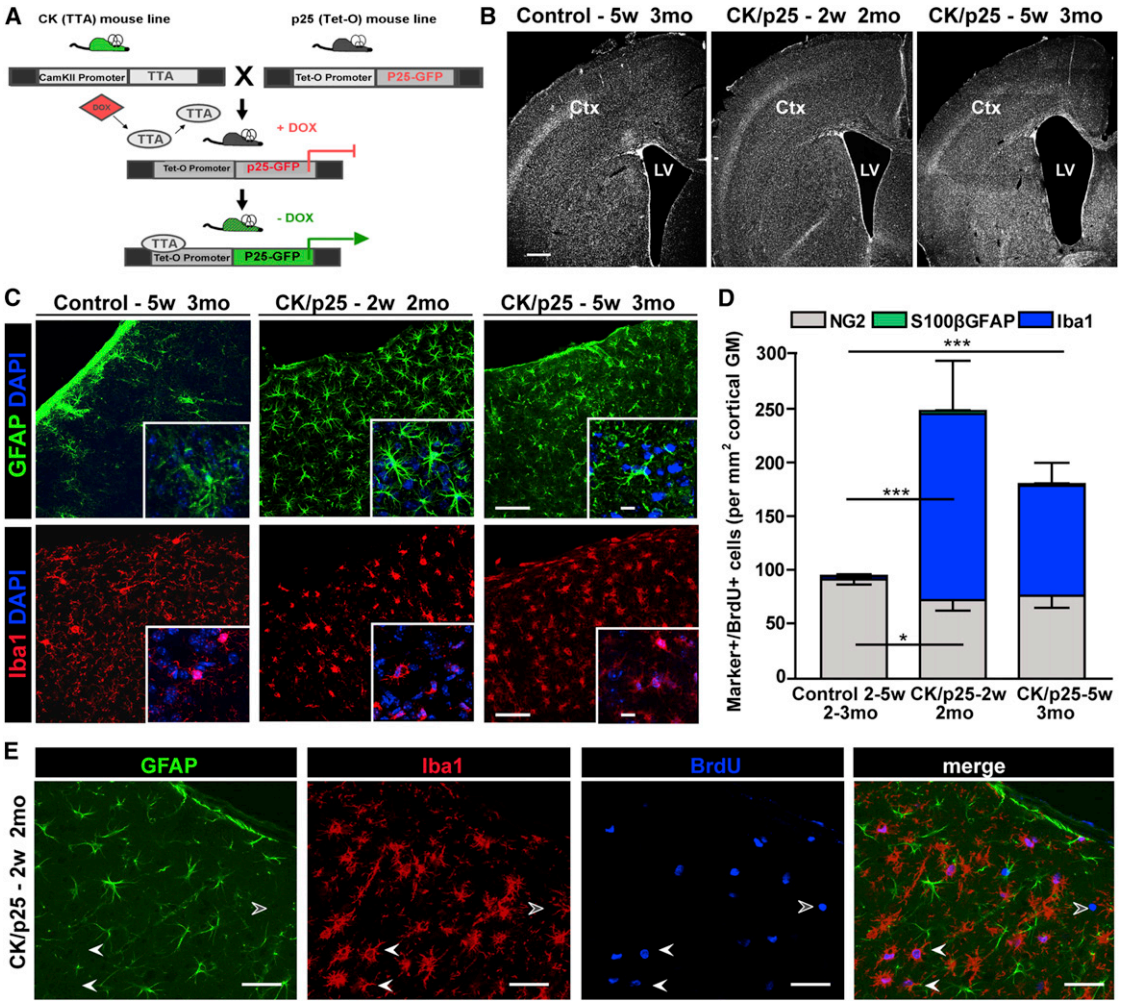

Figure 2. Reactive Gliosis and Proliferation in the Cerebral Cortex of the CK/p25 Mouse Model

(A) The diagram schematically depicts the constructs and regulatory strategy used to induce neuronal expression of p25. CK mice expressing the transactivator domain (TTA) under the CAMKII promoter were crossed with p25 mice expressing p25-GFP under the control of the Tet operon (Tet-O) promoter. Upon withdrawal of doxycycline (Dox), p25 is expressed in CAMKII-positive neurons in double-transgenic mice.

(B–E) Phenotypes of CK/p25 mice at various times after doxycycline withdrawal (B, C, and E), with (B) providing an overview and (C) and (E) showing astrocytes (GFAP+) and microglia (Iba1+) at higher magnifications (insets in C). Double-labeled cells are indicated by white arrowheads and single BrdU-labeled cells by empty arrowheads. The histogram in (D) provides a quantitative summary of the data, presented as mean (±SEM) per area in a section for three to seven animals. Significant differences relative to controls are indicated based on the p value. For additional analysis of the cerebral cortex of CK/p25 mice see Figure S2. Scale bars: (B), 200 μm; (C), 50 μm; insets: (C), 10 μm; (E), 20 μm.

To determine whether these reactive astrocytes also proliferate, we provided the DNA base analog BrdU in the drinking water for 2 weeks. The incidence of BrdU-labeled cells was significantly increased in APPPS1-3mo mice relative to controls, and their numbers further increased thereafter (Figure 1F). Surprisingly, however, only 2.7% of all BrdU+ cells also expressed the astrocyte markers GFAP and/or S100β (Figures 1G and 1H), and this population accounted for as little as 1.1% of all astrocytes in the GM of APPPS1-6mo mice, while up to 50% of astrocytes incorporate BrdU after stab wound (Buffo et al., 2008). Conversely, Iba1+ microglia showed a strikingly robust proliferative response, constituting the majority of proliferating cells (Figures 1G and 1H), while the remaining 40% of the proliferative glial cell pool in the GM of APPPS1-6mo mice was composed of NG2+ glia (Figures 1G and 1H).

Lack of Proliferation of Astrocytes or NG2 Cells after Widespread Neuronal Death Elicited by p25 Overexpression in the Cerebral Cortex

Given the virtual absence of cell death in APPPS1 mice (Rupp et al., 2011), we examined the glial reaction after neuronal overexpression of p25 induced by doxycycline withdrawal in CK/p25 mice at 6 weeks of age (Figure 2A, Cruz et al., 2003, 2006). Neuronal cell death became manifest within 2 weeks (CK/p25-2w) and resulted in profound shrinkage of the GM within 5 weeks (CK/p25-5w) (Figure 2B, Figures S2A and S2B). Reactive gliosis, as monitored by immunostaining for GFAP and Iba1, was clearly increased 14 days after p25 induction, while it is absent or less pronounced in controls (Figure 2C). Strikingly, the only glial cells to show increased proliferation were microglia (>100×), while neither astrocytes nor NG2 glia

increased their proliferation rate despite the massive neuronal cell death (Figures 2D and 2E).

As described previously (Simon et al., 2011), virtually all cells found to proliferate in the GM of controls for APPPS1 (6 months) and CK/p25 (~3 months) (Figures 1H and 2D) are NG2 glia, and their rate of proliferation decreases with age in controls (Figure 1F; see also Behrendt et al., 2013).

Invasive Injury Models Evoke Neurosphere Formation in Cells of Cerebral Cortex GM

While reactive astrocytes failed to proliferate in the above noninvasive models, they upregulated proteins also present in NSCs, such as nestin, the proteoglycan DSD1, or TNC (Figures S1 and S2C). This prompted us to probe their potential for neurosphere formation by isolating a defined volume of GM from the somatosensory cortex of noninjured controls, APPPS1 mice, and CK/p25 mice and plating the cells at clonal density (one to five cells/μl) for 14 days in vitro (div). Intact, uninjured GM gave rise to virtually no neurospheres, and only few neurospheres emerged from the GM of the APPPS1-6mo mice, although reactive gliosis was prominent at this age (Figures 3A and 3B). The few neurospheres that did form, however, exhibited the typical hallmarks of true stem cells: they could be passaged and were capable of self-renewal, as indicated by the formation of secondary neurospheres (Figure 3B). One-third of the neurospheres were also multipotent and generated neurons, astrocytes, and oligodendrocytes when exposed to differentiation conditions for 7 div (Figure 3C). This degree of multipotency is quite comparable to that of spheres generated from stab-wound-injured or laser-lesioned cerebral cortex (Buffo et al., 2008; Sirko et al., 2009). Because reactive astrocytes labeled by *GLAST*^{CreERT2}-mediated recombination generated most neurospheres after stab wound injury (Buffo et al., 2008), we crossed *GLAST*^{CreERT2}, a knockin mouse line that faithfully expresses CreERT2 in *GLAST*+ cells, and a GFP reporter line (Nakamura et al., 2006) with APPPS1 mice (Figure S3A) to trace the origin of the few neurospheres formed upon amyloidosis. At the dosage of tamoxifen used for fate mapping, this population consists mostly of astrocytes in the GM of the cerebral cortex (Figures S3A and S3B; Mori et al., 2006; Buffo et al., 2008; Robel et al., 2011b). All neurospheres derived from the cerebral cortex of 6-month-old *APPPS1;GLAST*^{CreERT2}*;CAG-eGFP* mice that received tamoxifen 30 days before they were sacrificed were GFP+ (Figure S3C). Thus, the few self-renewing and multipotent cells with neurosphere-forming capabilities that appear during chronic amyloidosis in the GM of the cerebral cortex must be derived from GLAST+ astrocytes. Contrary to our initial hypothesis that massive neuronal cell death should elicit a stronger NSC response, virtually no primary spheres, and no secondary neurospheres at all, formed from cells isolated from 3-month-old CK/p25 mice 5 weeks after doxycycline withdrawal (Figure 3B). Thus, both of these noninvasive models of pathology largely fail to elicit neurosphere formation and prompt a rather low proliferative response of the reactive astrocytes, the population responsible for generating most neurospheres.

Indeed, in injury models with higher rates of astrocyte proliferation, such as acute invasive injury, we observed a striking difference in the stem cell response. When cells were isolated from the tissue adjacent to a stab wound or the region that had been subjected to focal cerebral ischemia upon occlusion of the middle cerebral artery (MCAo) with a filament for 1 hr (Plesnila et al., 2004) at 3 days postinjury (3 dpi), we observed a 5-fold increase in the frequency of neurosphere formation compared to APPPS1 mice (Figures 3A and 3B; 45% of neurospheres from MCAo exhibited multipotency, data not shown). Thus, within 3 days after acute invasive injury, the neurosphere-forming response has reached a significant level, equivalent to one-fifth of the maximal incidence of stem cells obtainable from cells of the subependymal zone (SEZ). In models of chronic noninvasive injury, in contrast, such a response is virtually or totally absent.

These models may either fail to elicit a latent stem cell potential or, alternatively, reactive glia/astrocytes may be prevented from manifesting such potential by inhibitory signals, such as aberrant Notch signaling due to the mutant form of presenilin present in the neurons of APPPS1 mice (De Strooper et al., 1999; Radde et al., 2006; Veeraraghavalu et al., 2010) or the toxicity of Aβ amyloid. To address the first possibility, APP23 mice overexpressing only mutant APP, but not aberrant PS1 (Sturchler-Pierrat et al., 1997), were investigated at a comparable stage of amyloidosis, at 12 months of age (Boncristiano et al., 2005; Radde et al., 2006; Sturchler-Pierrat et al., 1997). Cells isolated from these mice gave rise to comparably small number of neurospheres (Figure S3D), indicating that this trait cannot be attributed to the aberrant PS1 expression in APPPS1 mice. Next, APPPS1-9mo mice were subjected to stab wounding, and here we detected a significant increase in the number of primary and secondary neurospheres generated from cells obtained at 3 dpi compared to age-matched APPPS1 mice (Figure 3D). Moreover, the number of neurospheres formed was not significantly different from that observed when cells from age-matched control mice lacking amyloidosis were tested (Figure 3D). These findings indicate that cells with the potential to form neurospheres are still present in APPPS1 mice, but are largely impervious to activation by the signals elicited by amyloid plaque deposition.

Interestingly, in the course of the above experiments, we noted that age had a strong influence on the rate of neurosphere formation after stab wound injury. Cells isolated at either 3 or 5 dpi from the cortex of 6- or 9-month-old mice subjected to stab wounding gave rise to 2- to 3-fold fewer neurospheres than cells obtained from 3-month-old mice (Figure 3E). However, irrespective of age, stab wound injury always elicits the appearance of a significantly higher number of neurospheres than does amyloidosis (Figure 3E), and no neurospheres have yet been obtained from the cortex of APPPS1-3mo mice, suggesting that the degree of amyloidosis and reactive gliosis at this point is too low to elicit any neurosphere formation at all (Figure 3E).

Levels of SHH in the Cerebral Cortex Rise after Invasive Injury

The experiments described above uncovered a profound difference in the incidence of astrocyte proliferation and in vitro neurosphere formation elicited by invasive (stab wound, MCAo) versus noninvasive injury, such as amyloidosis or p25-induced neuronal death. To gain insight into the molecular basis for this differential response, we focused on pathways previously suggested to regulate the proliferation of reactive glia and

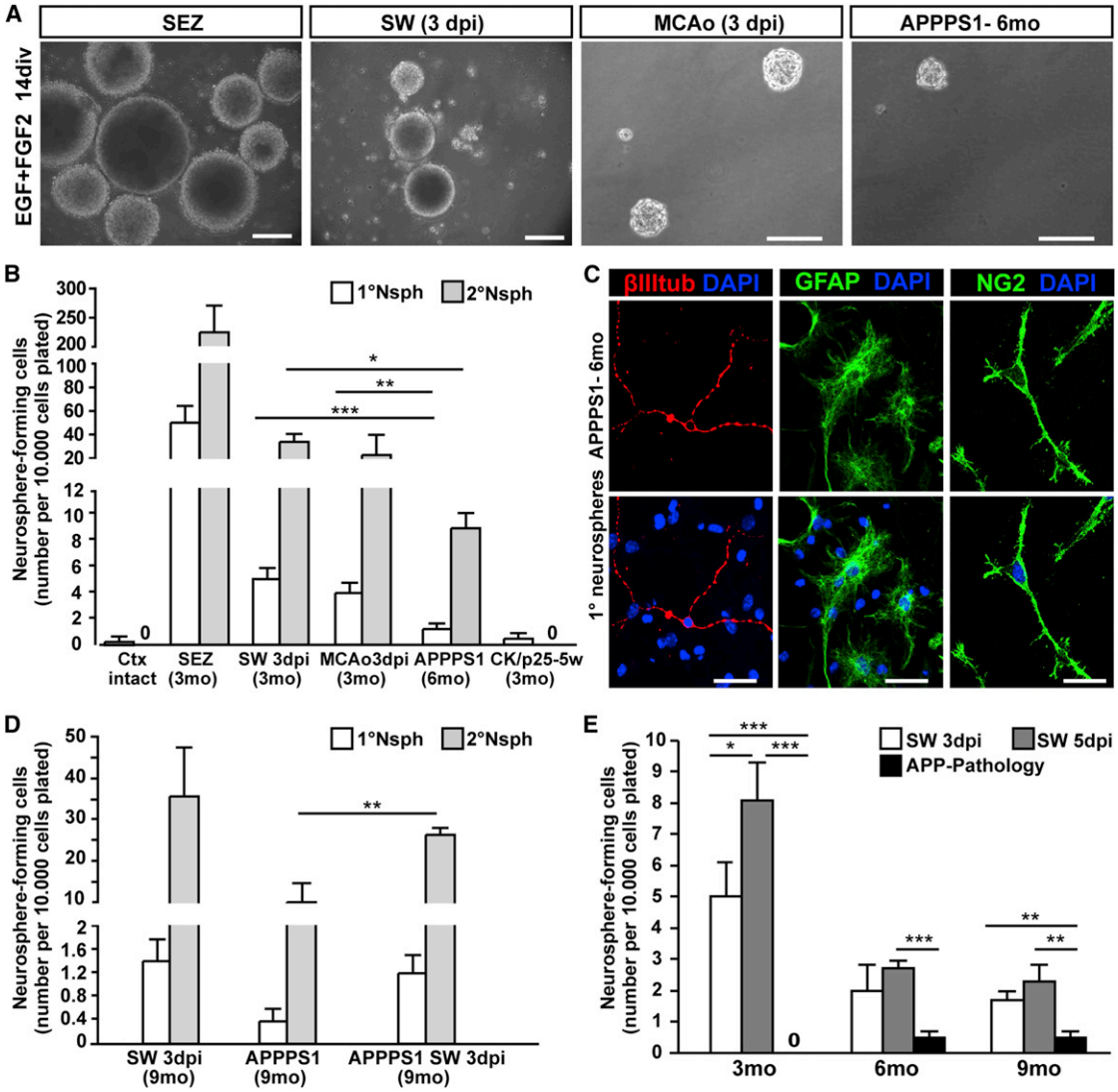

Figure 3. Neurosphere Formation by Cells Isolated from Different Injury Models

(A) Examples of neurospheres formed by cells of the SEZ, the cerebral cortex 3 days after stab wound (SW) or after induction of MCAo, or the cortex of APPPS1-6mo mice after 14 days in culture. The data for all injury models tested are depicted in (B). (C) Representative micrographs show cells derived from primary APPPS1-6mo neurospheres, differentiated for 7 days, and immunostained for the cell-type-specific markers indicated. Histograms in (B) and (D) depict the numbers of primary (1°, white bars) and secondary (2°, gray bars) neurospheres (Nsph) per 10,000 cells isolated. The histogram in (E) shows the numbers of neurospheres generated by cells from stab-wounded or APPPS1 animals at different ages. All data are means (±SEM) per independent experiment, and significant differences are indicated based on the p value. Number of independent experiments analyzed for (B): SEZ, n = 6; GM of intact Ctx, n = 3; lesioned Ctx after SW, n = 8, or MCAo, n = 11; APPPS1, n = 8; CK/p25, n = 3; for (D): n = 3 for each condition; for (E): n = 3, per group and time point after injury. For additional analysis of neurosphere formation, see Figure S3. Scale bars: (A), 100 μm; (C), 20 μm.

measured levels of phosphorylated STAT3 (pSTAT3) and c-Jun (pc-Jun) (Figure S4) and levels of SHH (Amankulor et al., 2009; Gadea et al., 2008; Robel et al., 2011a; Sofroniew, 2009; Tsuda et al., 2011). Only levels of SHH were found to correlate with the proliferative and stem cell response. Both forms of SHH, the monomer (25 kDa) and the multimer (52 kDa), were detected in the GM of the cerebral cortex and their levels increased significantly on the ipsilateral side between 1 and 5 dpi (Figures 4A and 4B). Intriguingly, a similar increase was observed 3 days after MCAo (Figure 4B), while no noteworthy changes in amounts of SHH were detected in the cerebral cortex of APPPS1, CK/p25 (Figures 4C and 4D), or APP23 mice (Figure S3E). Taken together, these data demonstrate that SHH is upregulated specifically in injury models that display a significant increase in macroglia proliferation and neurosphere formation in response to insult.

To determine the source of the increase in SHH after stab wound injury, we used immunostaining and in situ hybridization. In accordance with previous data (Alvarez et al., 2011; Amankulor et al., 2009; Garcia et al., 2010; Traiffort et al., 1999), we detected SHH mRNA and protein in neurons of the cerebral cortex, both in the absence of injury and in the region around

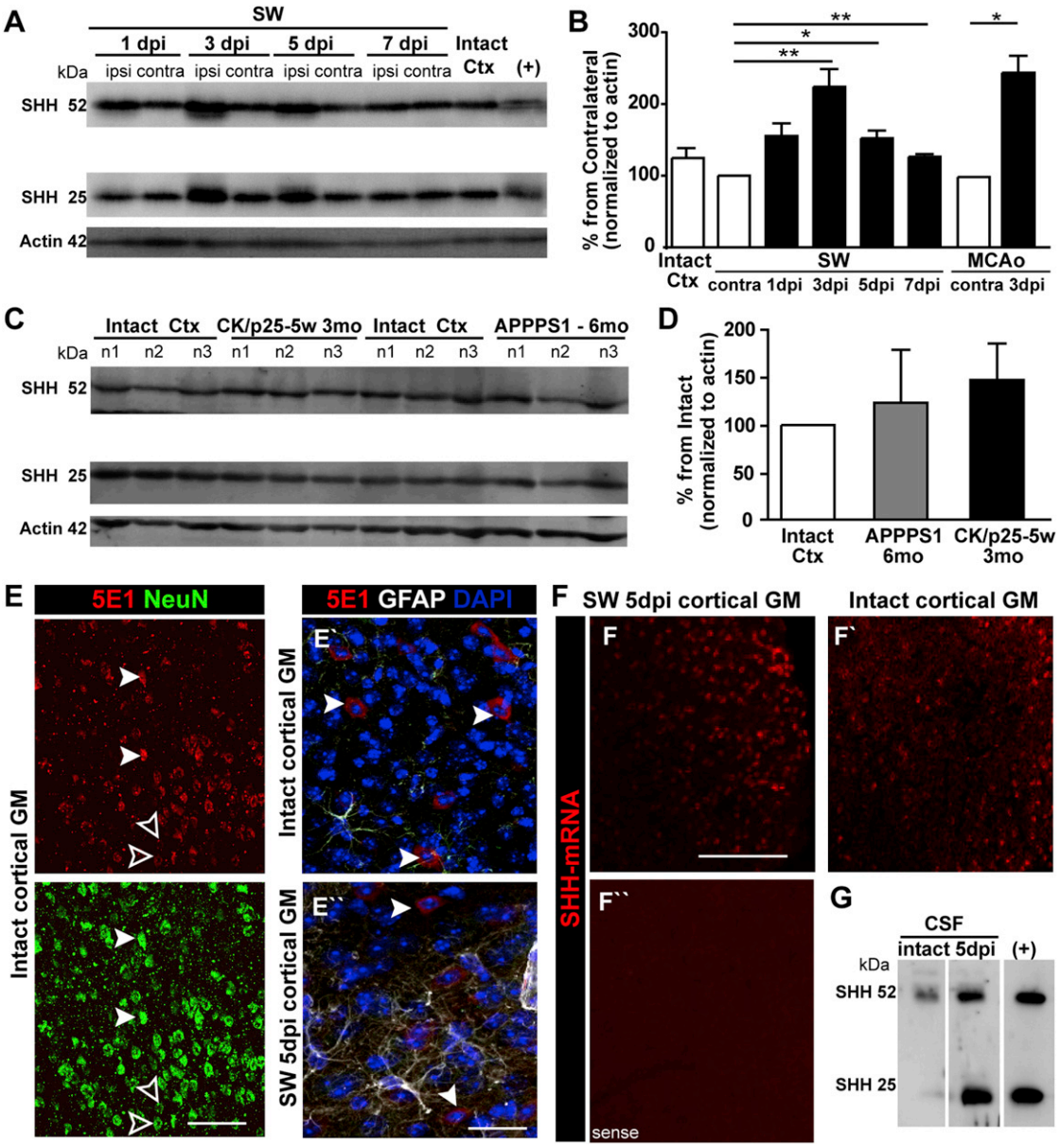

Figure 4. SHH Expression in the Cerebral Cortex of Different Injury Models

(A–D) Western blot analysis with mAb 5E1 of SHH protein in tissue lysates of intact somatosensory cerebral cortex, or the cortical region ipsilateral (ipsi) or contralateral (contra) to a stab wound, isolated at the indicated times (days post injury, dpi) after infliction of the injury (A) or from the mouse lines indicated in (C). Recombinant mouse SHH protein was used as a positive control (+). The histograms in (B) and (D) depict the quantitative analysis of western blots by densitometry normalized to the actin loading control and the contralateral (B) or intact cortex (D) (intact Ctx, n = 9; n = 3 per time point after SW; MCAo, n = 3; APPPS1, n = 3; CK/p25, n = 3). All data are mean (±SEM) per independent experiment, and significant differences are indicated based on the p value. Micrographs in (E) show immunostaining for SHH (5E1), GFAP, and NeuN. SHH+ cells are indicated by arrowheads and SHH− cells by empty arrowheads. Micrographs in (F) show SHH mRNA in control and stab-wounded (5 dpi) hemispheres hybridized with antisense (F and F′) and sense (F″) probes (for FISH see Bozoyan et al., 2012) and (G) shows a western blot of CSF lysates prepared 5 dpi or from intact, noninjured mice. For additional analysis, see Figures S3 and S4. Scale bars: (E), 75 μm; (E′ and E″), 30 μm; (F–F″), 50 μm.

the stab wound (Figures 4E and 4F). Immunoreactivity and mRNA was also detected in some astrocytes and endothelial cells, especially after injury, but these cells made only a minor contribution to the total signal (data not shown). Because extraneural fluids infiltrate the brain parenchyma after invasive injury, we checked the cerebrospinal fluid (CSF), and found significant amounts of SHH (Figure 4G), suggesting that extraneural sources contribute to the higher SHH levels seen in the brain after invasive injury. It should be noted here that, while the stab wound does not penetrate the ventricles, it does disrupt the subarachnoid space overlying the cerebral cortex, which contains CSF.

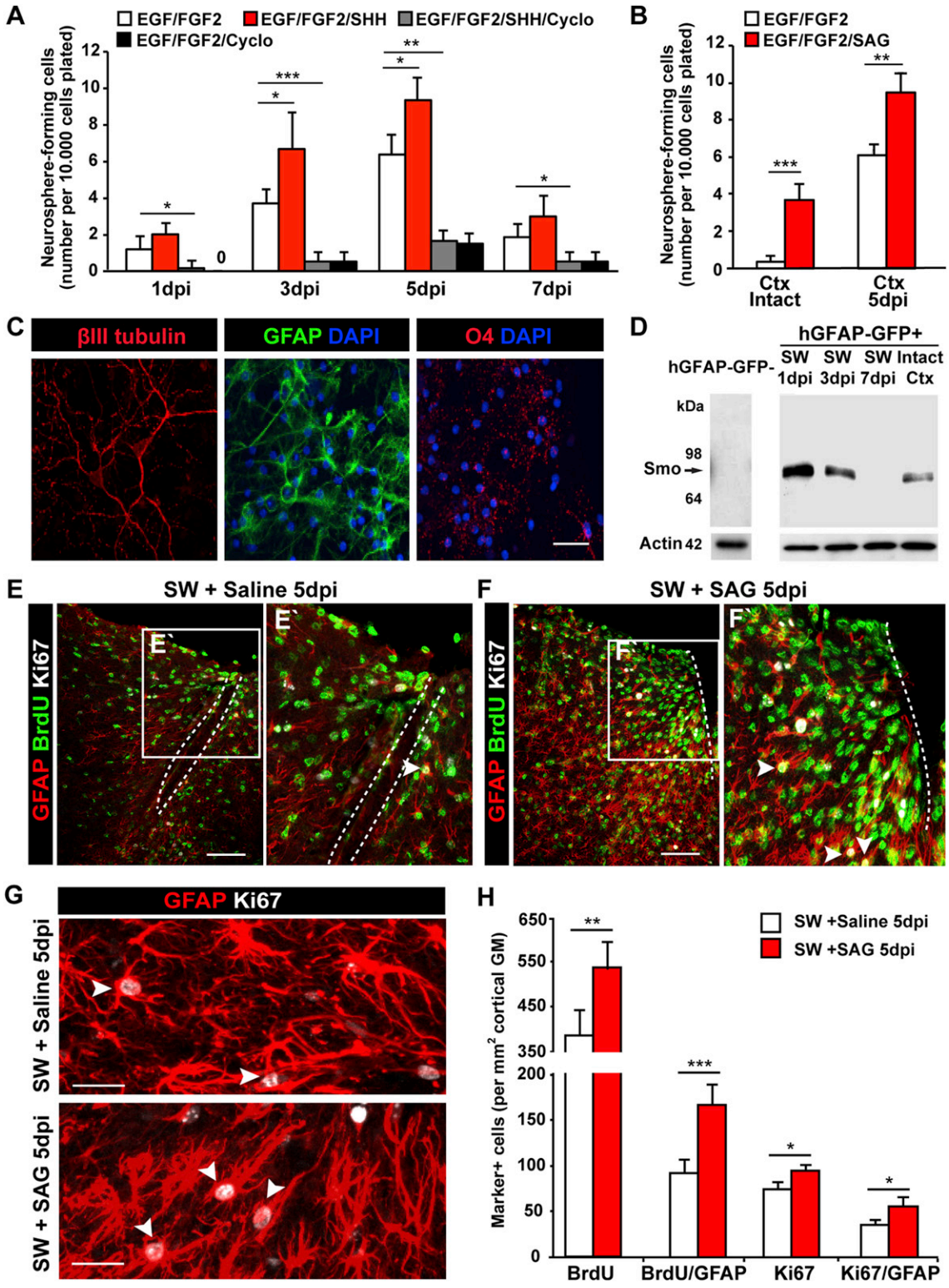

Figure 5. Effects of Application of the SHH Agonist SAG In Vitro and In Vivo

Histograms in (A) and (B) depict the number of neurospheres generated from GM cells isolated 1, 3, 5, and 7 dpi (n = 3 per time point) and cultured under the conditions indicated by the color of the bars. (C) Neurosphere-derived cells isolated from the intact cerebral cortex and cultured in SHH-, EGF-, and FGF2-containing medium showed their multipotency by differentiating into βIII tubulin+ neurons, GFAP+ astrocytes, and O4+ oligodendrocytes. (D) Western blot analysis of the SHH transducer Smoothened (Smo) in lysates of GFP+ and GFP− cells from intact or stab-wounded cerebral cortex of *hGFAP-eGFP* mice purified by FACS. Micrographs in (E–G) depict examples of immunostaining with the indicated antibodies of sections obtained from SAG- (F and G) or saline-treated

(legend continued on next page)

SHH Signaling Is Necessary and Sufficient for the In Vitro Stem Cell Response after Injury

In order to determine the functional significance of SHH for the stem cell response of reactive glia, we first asked whether addition of SHH protein to the in vitro neurosphere assay affected the capacity of isolated cells to generate neurospheres. Quantitative assessment of cultures prepared from cortical GM at 1, 3, 5, and 7 dpi revealed a significant increase in neurosphere formation in the presence of 5 nM SHH in cultures derived from 3 and 5 dpi cells compared with control cultures (Figure 5A). This effect could be blocked by the addition of cyclopamine (5 μM) (Figure 5A), a known inhibitor of SHH signaling (Chen et al., 2002). Because cyclopamine also interfered with neurosphere formation in cultures to which no SHH was added, these data confirm the release of endogenous SHH by neurosphere cells under these culture conditions (Gabay et al., 2003). The specificity of the effect of added SHH and its blockade by cyclopamine was further corroborated by experiments with SAG, which activates the SHH signal transducer Smoothened (Smo) (Frank-Kamenetsky et al., 2002). Thus, supplementation of cultures with SAG significantly enhanced neurosphere formation by cells surrounding the stab wound site (Figure 5B). Strikingly, both SHH (data not shown) and SAG were sufficient to elicit neurosphere formation from GM that had not been subjected to injury (Figure 5B). Thus, activation of the SHH pathway in vitro is sufficient to enable formation of multipotent neurospheres (Figure 5C) by cells isolated from GM of the cerebral cortex of adult mice, even in the absence of prior insult.

SHH-Mediated Signaling Promotes Proliferation of Reactive Astrocytes In Vivo

Since neurosphere-forming cells originate from reactive astrocytes, we purified hGFAP-eGFP+ reactive astrocytes by fluorescence-activated cell sorting (FACS) and found Smo to be highly enriched in reactive astrocytes with expression level increased at 1 dpi, while it was virtually undetectable in cell lysates derived from GFP− cells (Figure 5D). These findings indicate that reactive astrocytes not only constitute the major source of neurosphere-forming cells but are also capable of responding to the increased levels of SHH observed in injured tissue. This prompted us to investigate whether direct activation of Smo by SAG is also sufficient to enhance the proliferative response of reactive astrocytes in vivo. After daily treatment with SAG (0.15 mg/10 g body weight) and addition of BrdU in the drinking water for 5 days after stab wounding, the number of BrdU+ cells around the injury site had increased significantly relative to controls (Figures 5E, 5F, and 5H). Moreover, there was a significant rise in proliferating reactive astrocytes, as measured by BrdU incorporation over the 5 days (BrdU+/GFAP+) and reflected in the number of astrocytes still proliferating at 5 dpi (labeled by Ki67) (Figures 5G and 5H). These data demonstrate that in vivo levels of SHH are not saturating and that glial cell proliferation, as well as neurosphere formation, can be further boosted by treatment with agonists of Smo. This finding is of particular relevance in light of the decrease in the endogenous response with aging.

It seems likely that signaling molecules other than SHH are also relevant for the proliferative and stem cell response of reactive astrocytes. We therefore wished to assess the relative contribution of the SHH pathway to the overall process. To do so, we injected cyclopamine or 2-hydroxypropyl-β-cyclodextrin (HBC) (vehicle) intraperitoneally (i.p.) daily after stab wound injury and isolated the cells surrounding the injury site for the neurosphere assay as described above. Strikingly, virtually no neurospheres could be generated from cells obtained from cyclopamine-treated mice, while vehicle injection did not perturb the formation of neurospheres after stab wounding (Figure 6A). Real-time qRT-PCR of astrocytes isolated from *hGFAP-eGFP* mice at 5 dpi revealed that cyclopamine significantly decreased levels of mRNAs for Smo, Ptch1, SHH, Gli1–3, and their effector cyclin D1 (Figure 6B; see also Figure S5 for cell death analysis). These data argue that the drastic reduction in proliferation of reactive astrocytes from cyclopamine-treated mice is largely attributable to interference with SHH signaling.

However, cyclopamine may well affect cells other than reactive astrocytes, and could thereby exert indirect effects via other signaling pathways. To determine the effect of direct SHH signaling to astrocytes, we examined whether removal of its transducer from astrocytes affected their proliferative and stem cell response after stab wounding. To this end, we conditionally deleted the *Smo* gene (Long et al., 2001) in astrocytes by $GLAST^{CreERT2}$-mediated recombination, monitored by the GFP reporter as described above. Animals heterozygous for $GLAST^{CreERT2}$, positive for the GFP reporter, and homozygous ($GLAST^{CreERT2}$;$Smo^{fl/fl}$;*CAG-eGFP*) or negative ($GLAST^{CreERT2}$;$Smo^{+/+}$;*CAG-eGFP*) for the floxed *Smo* allele were exposed to tamoxifen at 3 months of age and were subjected to stab injury 3 months later. A large proportion of the reactive astrocytes identified by GFAP expression at 5 dpi had undergone recombination, as indicated by the presence of the GFP reporter. In control ($Smo^{+/+}$) animals, 53.4% ± 8.9% of GFAP+ cells are GFP+, while the corresponding value for $Smo^{fl/fl}$ mice is 59.3% ± 7.2%. Strikingly, selective deletion of *Smo* in $GLAST^{CreERT2}$;$Smo^{fl/fl}$;*CAG-eGFP* animals significantly reduces the degree of proliferation (fraction of Ki67+ cells) of the recombined GFP+ cells to one-third of that seen in the controls ($GLAST^{CreERT2}$;$Smo^{+/+}$;*CAG-eGFP*) that received the same dose of tamoxifen at 3 months (Figures 6F–6H). Hence, these data demonstrate a pronounced direct effect of SHH signaling via the Smo transducer in astrocytes, with this pathway accounting for 60% of the increase in their proliferative activity after stab wound injury. Because we cannot distinguish between GFP+ cells that carry one or two recombinant floxed alleles, and because many cells may still have remnant levels of Smo, the effects might well be even greater if Smo could be eliminated from all astrocytes. Notably, the stem cell response (monitored by neurosphere formation) obtained from cells surrounding the stab wound in $GLAST^{CreERT2}$;$Smo^{fl/fl}$;*CAG-eGFP* mice was also reduced by about two-thirds

(E and G) animals. The insets (E′) and (F′) show higher magnifications and the white arrowheads indicate double- or triple-labeled cells. The dashed lines indicate the site of injury. Quantitative analysis of these experiments is depicted in the histograms in (H). All data are represented as mean (±SEM) per independent experiment, and significant differences are indicated based on the p value. For additional analysis see Figure S5. Scale bar: (C), 50 μm; (E and F), 100 μm; (G), 30 μm.

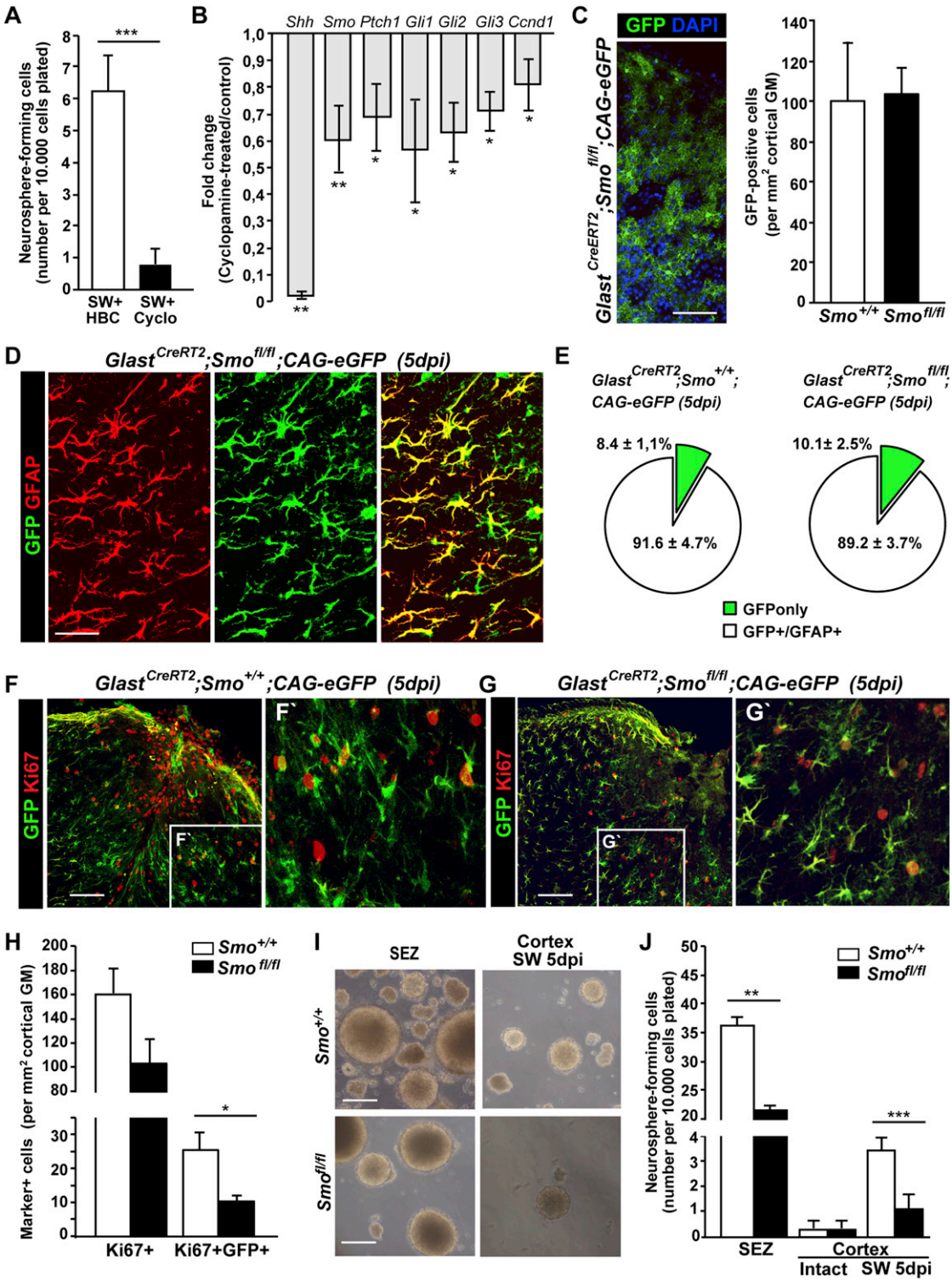

Figure 6. Effects of Inhibition/Deletion of Smoothened on Astrocyte Proliferation In Vivo and Stem Cell Properties In Vitro

(A) Numbers of neurospheres formed by cells isolated after stab wounding followed by three daily injections with either the diluent HBC (SW+HBC) or cyclopamine (SW+Cyclo, n = 3 for each condition).

(B) Levels of the indicated mRNAs in GFP+ cells purified by FACS from cyclopamine-treated *hGFAP-eGFP* mice at 3 dpi, as determined by qRT-PCR, shown relative to values for SW+HBC controls.

(C) Recombination efficiency, as monitored by the incidence of GFP+ cells, in the intact cerebral cortex of *GLAST^{CreERT2};Smo$^{+/+}$;CAG-eGFP* and *GLAST^{CreERT2};Smo$^{fl/fl}$;CAG-eGFP* mice exposed to tamoxifen at 3 months of age and analyzed 3 months later (n = 3).

(legend continued on next page)

compared to control (*Smo*$^{+/+}$) animals (Figures 6I and 6J). Conversely, neurosphere formation from the SEZ of *GLAST*^{CreERT2};*Smo*$^{fl/fl}$;*CAG-eGFP* mice was reduced by only about 30%, suggesting that signals other than SHH may be of more relevance in the SEZ than in the cortex after stab injury. These data further corroborate the specificity and efficiency of *Smo* deletion by *GLAST*^{CreERT2} and suggest a direct effect of SHH signaling on the proliferative response of reactive astrocytes in vivo and on their stem cell potential in vitro.

DISCUSSION

Reactive gliosis occurs as a widespread reaction to brain damage or injury. Here we have demonstrated profound differences in the nature of this reaction to invasive versus noninvasive injury conditions. While aspects of morphological activation, such as hypertrophy, and upregulation of characteristic proteins, like GFAP, occurred in all the injury models examined here, pronounced differences were observed in the proliferative responses of distinct glial subsets depending on the type of injury. In contrast to microglia, which proliferated at high frequency in all pathology models and at all different ages examined here, reactive astrocytes proliferate very little in chronic amyloidosis (1% of astrocytes; see also Kamphuis et al., 2012) and not at all upon p25-induced neuronal cell death. This low degree of proliferation was observed despite pronounced hypertrophy of GFAP+ astrocytes accompanied by upregulation of proteins also expressed in NSCs (Gates et al., 1995), such as nestin, DSD1, and TNC (Robel et al., 2011a) (Table 1). Thus, upregulation of these proteins neither reflects the acquisition of in vitro stem cell properties nor is associated with a robust in vivo proliferative response. In contrast, both the proliferative response and the capacity for neurosphere formation was markedly increased following stab wound or ischemic injury (see Table 1 and Buffo et al., 2008; Simon et al., 2011; Denes et al., 2007). Most striking is the absence of any proliferative reaction by astrocytes or NG2 glia in the presence of the extensive neuronal death induced by p25 overexpression in neurons. Thus, neuronal cell death does not trigger proliferation of macroglia, despite their intricate contacts with neurons at synapses. This concept of a distinct reaction of macroglial cell proliferation is further supported by recent data from the zebrafish model, which reveal differences in proliferation of Olig2 glia under different injury conditions, while division of microglia increases under all lesion conditions (Baumgart et al., 2012; Kroehne et al., 2011; März et al., 2011).

The Stem Cell Response of Astrocytes Is Injury Dependent

The differential proliferative reaction of macroglial cells correlates with the emergence of neurosphere-forming cells in the injury models examined here. We consider this to be a stem cell response because cells activate the capacity to self-renew and generate all three CNS cell types in vitro. This shows that they acquire NSC potential, even though not all of these features can be realized in vivo. While the stem cell response of reactive glia is highest under conditions of acute injury, such as stab wounding and MCAo (Lang et al., 2004; Shimada et al., 2012), it is significantly reduced in models of amyloidosis. This was the case for cells isolated from the cerebral cortex of APPPS1 as well as APP23 mice, ruling out potential side effects of PS1 expression in neurons of APPPS1. Importantly, stab wound injury in mice with intense amyloidosis could still elicit the stem cell response to a similar extent as in control mice, clearly demonstrating that a lack of inducing signals, rather than toxicity or damage to the reactive glia, is responsible for the limited stem cell response.

Strikingly, the stem cell response was entirely absent in the case of the massive neuronal cell death elicited in the cerebral cortex by induced p25 overexpression. Not a single self-renewing neurosphere was generated from cortical cells isolated from such mice, nor could any reactivation of astrocyte proliferation be observed 2 or 5 weeks after p25 overexpression induced by doxycycline withdrawal. Because this covers the time of onset of neuronal death and reactive gliosis, it is unlikely that the stem cell reaction occurred at an earlier stage. Moreover, BrdU was supplied in the drinking water for the entire period after doxycycline withdrawal, but we still failed to detect any proliferation of astrocytes, the neurosphere-forming cells. Thus, the death of many neurons in the cerebral cortex is not sufficient to elicit a stem cell response from reactive astrocytes.

SHH Is Necessary and Sufficient to Elicit a Stem Cell Response from Reactive Astrocytes

Because these results suggested that a lack of inducing signals is responsible for the failure of reactive astrocytes to display proliferative and stem cell responses in noninvasive injury models, both the low levels of SHH observed in the cortex after profound amyloidosis or p25-induced cell death and the significantly elevated levels of SHH seen after stab wound injury and stroke, together with SHH's presence in endogenous stem cell niches (Lai et al., 2003; Machold et al., 2003), provided a hint that SHH might play a positive role in the stem cell reaction. Notably, neurons, astrocytes, and choroid plexus cells have been described as sources of SHH (Alvarez et al., 2011; Amankulor et al., 2009; Garcia et al., 2010; Traiffort et al., 1999), and the presence of considerable amounts of SHH in CSF (Huang et al., 2009) may help to explain why invasive injuries result in the accumulation of significant levels of the signal (Amankulor et al., 2009; Androutsellis-Theotokis et al., 2006), while the noninvasive models, such as amyloidosis or p25 induced neuronal death, do not. Interestingly, SHH is also present in human

(D–H) Representative micrographs of cortical sections obtained from mice of the indicated genotypes and analyzed for the indicated antigens (D, F, and G). Quantitative summaries of the data are shown in (E) and (H).

(I) Micrographs of neurospheres generated from cells isolated from the subependymal zone (SEZ) or the GM of stab-wounded cerebral cortex of *GLAST*^{CreERT2};*Smo*$^{+/+}$;*CAG-eGFP* and *GLAST*^{CreERT2};*Smo*$^{fl/fl}$;*CAG-eGFP* mice.

(J) Data from (I), quantified.

All data are plotted as mean (±SEM) per independent experiment (n = 3 per condition), and significant differences are indicated based on the p value. For additional analysis see also Figure S5. Scale bars: (C) and (I), 150 μm; (D), 100 μm; (F) and (G), 120 μm.

Table 1. Summary of Reactive Gliosis in Distinct Models of AD Pathology and Invasive Injury

Cell-Type-Specific Reaction (in Cortical GM)		Intact CNS	Alzheimer Pathology		Stab Wound Injury, 5 dpi
			APP	CK/p25	
Cell morphology	astrocytes	radiating fine processes	hypertrophy of cell soma/processes	hypertrophy of cell soma/processes	hypertrophy of cell soma/processes
	NG2+ glia	highly branched, fine processes	thicker processes, enlarged soma	highly branched, fine processes	thicker processes, enlarged soma
	microglia	highly branched, fine processes	few processes, hypertrophy	few processes, hypertrophy	few processes, hypertrophy
Proliferative capacity	astrocytes	nonproliferative (<0.5%)	low contribution to proliferative pool (2.7% ± 0.2%)	low contribution to proliferative pool (0.9% ± 0.3%)	high contribution (22.5% ± 1.6%)
	NG2+ glia	proliferative (99%)	high contribution (41.1% ± 9%)	high contribution (48.9% ± 7.7%)	high contribution (24.8% ± 3.6%)
	microglia	nonproliferative (<0.5%)	highest contribution (56.2% ± 7.4%)	highest contribution (50.1% ± 2.9%)	highest contribution (46.2% ± 1.6%)
Stem cell response	neurosphere-forming capacity	no (<0.001%)	yes (0.007% ± 0.002%)	virtually none (0.003% ± 0.003%)	yes (0.081% ± 0.004%)
	multipotency (glial: neuronal)	no (glial)	yes (2:1)	yes (2:1)	yes (2:1)
	self-renewal	no	yes (0.126% ± 0.027%)	no	yes (0.366% ± 0.059%)
	activity of SHH pathway	basal level	not significantly upregulated	not significantly upregulated	significantly upregulated

Proliferative capacity refers to the relative contribution of each of the different glial cell types (mean ± SEM) to the total population of BrdU+ cells determined per 1 mm^2 of the cortical GM in brain sections after double-immunostaining with BrdU and cell-type-specific markers (NG2 for NG2-expressing oligodendroglia, GFAP/S100β for astroglia, and Iba1 for microglia). The neurosphere-forming capacity is expressed as the percentage (mean ± SEM) of neurosphere-generating cells per 10,000 cells obtained from the somatosensory cortex of the adult mouse brain. The self-renewal capacity refers to the fraction of the neurosphere-forming cells per 10,000 cells obtained from dissociated primary neurosphere cultures.

CSF and plasma (El-Zaatari et al., 2012), implying similar access to the brain after invasive injury in patients.

Importantly, we were able to demonstrate that SHH signaling is both necessary and sufficient to promote the proliferative response in vivo and neurosphere formation in vitro by acting directly on reactive astrocytes. Astrocytes express the SHH transducer Smoothened, and its selective deletion in these cells impairs their proliferation in vivo and their potential to form neurospheres in vitro. Notably, early postnatal deletion of Smoothened in astrocytes also induced a partially reactive phenotype with GFAP upregulation but no evidence for astrocyte proliferation (Garcia et al., 2010). Taken together, these results imply a U-shaped model for the action of SHH, with both too low and too high levels of SHH signaling activating reactive gliosis and higher levels triggering an additional proliferative response. Alternatively, SHH signaling may specifically interact with other pathways, e.g., Notch or BMP signaling (Androutsellis-Theotokis et al., 2006; Sehgal et al., 2009) at early postnatal stages to drive astrocyte maturation to completion.

Interestingly, addition of SHH or the Smo agonist SAG in vitro and in vivo not only boosted the proliferative response of reactive astrocytes as well as their neurosphere-forming capacity, but was even sufficient to elicit neurosphere formation from cells of the cerebral cortex GM in the absence of any injury. This is particularly important with regard to the aging-related decline in the proliferative and stem cell response upon injury. Interestingly, intrathecal application of SHH resulted in significant improvement of neurological outcome in a rat model of stroke (Bambakidis et al., 2012). These beneficial effects relate to the pleiotropic effects of SHH, which promotes blood-brain barrier integrity and anti-inflammatory effects (Alvarez et al., 2011), has a neuroprotective action (Hashimoto et al., 2008), and boosts proliferation in endogenous neurogenic niches and in the cerebral cortex after injury (Sims et al., 2009; Machold et al., 2003; Lai et al., 2003). Finally, SHH activity has been implicated in regeneration in many models (for review see Antos and Tanaka, 2010; Stoick-Cooper et al., 2007), suggesting that it has a widespread positive effect on wound healing and repair. Thus, the pleiotropic actions of SHH are likely to exert several beneficial effects after brain injury, in addition to promoting the stem cell response of reactive gliosis.

Indeed, it is important to bear in mind that the discovery of a particularly plastic and immature set of reactive astrocytes is of great significance, not only because these cells may be more easily persuaded to adopt desirable fates (for review see Robel et al., 2011a; Shimada et al., 2012), but also because more immature glia, such as radial glial cells, may have many other beneficial aspects, such as promoting neurite outgrowth and synapse formation, while scar-forming reactive astrocytes often inhibit it, thereby restricting rewiring after brain injury (Fitch and Silver, 2008). Taken together, our work highlights key differences in the proliferative and stem cell response of reactive glia in different injury paradigms and has identified a key signaling pathway, which provides a novel perspective for efforts to stimulate this endogenous stem cell response for therapeutic purposes.

EXPERIMENTAL PROCEDURES

Animals

APPPS1 mice (Radde et al., 2006) were maintained on a C57Bl/6 background (Charles River Laboratories; Sulzfeld, Germany) and C57Bl/6 mice were used as controls. For genetic tracing of astrocytes, APPPS1 mice were crossed with *GLAST*^{CreERT2} mice (Mori et al., 2006) and the *CAG-eGFP* reporter line (Nakamura et al., 2006). Recombination was induced by administration of tamoxifen as previously described (Mori et al., 2006). For selective deletion of *Smo* in astrocytes, homozygous mice carrying floxed *Smo* alleles (*Smo*$^{fl/fl}$, Long et al., 2001), *GLAST*^{CreERT2} mice (Mori et al., 2006), and the *CAG-eGFP* reporter line (Nakamura et al., 2006) were used. Genotypes were determined by PCR using primers listed in the Supplemental Information. CK/p25 animals (Cruz et al., 2003) were raised on doxycycline (0.05 g/l doxycycline/1.5% sucrose in drinking water) until 6 weeks of age. Littermates that did not harbor any transgene were used as controls and exposed to doxycycline in the same way as experimental animals.

Surgical Procedures

Unilateral stab wound (0.7 mm deep and 1 mm long) was performed in the somatosensory cortex of C57Bl/6 mice as previously described (Buffo et al., 2008; Simon et al., 2011). For focal ischemia, adult C57Bl/6 male mice were subjected to transient MCAo for 60 min according to the intraluminal filament model (Plesnila et al., 2004). I.p.) injections of cyclopamine (10 mg/kg, Sigma Aldrich) diluted in HBC, (Sigma Aldrich) were performed every 24 hr while control animals received injections of HBC only. SAG (Calbiochem) was administered orally (0.15 mg in 0.5% methylcellulose/0.2% Tween80 per 10 g body weight) once a day for 5 days. CSF was sampled from the cisterna magna using a glass capillary and was microscopically inspected for blood contamination. All experimental procedures were performed in accordance with the animal welfare policies of, and approved by, the State of Bavaria.

Immunohistochemistry

After transcardial perfusion, brains were cryoprotected, and sections (30 μm) were processed for immunohistochemistry as previously described (Simon et al., 2011) with the antibodies listed in the Supplemental Information. Proliferating cells were labeled with BrdU (Sigma Aldrich) added to the drinking water (1 mg/ml water containing 1% sucrose) for 5 or 14 consecutive days. BrdU incorporation was monitored in free-floating sections pretreated with 0.01 M sodium citrate (pH 6) at 95°C for 20 min.

Neurosphere Culture

Neurosphere cultures were prepared as previously described (Buffo et al., 2008) using a volume of tissue punched (∅ 0.35 cm) from the lesioned and non-lesioned areas of the (stabbed or MCAo-injured) somatosensory cerebral cortex or the corresponding anatomical areas of APPPS1 and CK/p25 mice. After removal of meninges and white matter, GM cells were plated at a density of one to five cells/μl in 600 μl of neurosphere medium with FGF2 and EGF (both at 20 ng/ml, Invitrogen). In parallel sets, SHH (5 nM, R&D), cyclopamine (5 μM, Sigma Aldrich), or SAG (0.5 μM, Calbiochem) was added at the beginning of the experiment only. The number of neurospheres was quantified after 14 div and individual neurospheres were assessed for self-renewal or differentiation as described in Buffo et al. (2008).

Western Blot

The same tissue volume (∅ 0.35 cm) or 1 μl of CSF was used for western blot analysis with the antibody 5E1 (Developmental Studies Hybridoma Bank, University of Iowa, IA) as described by Ohlig et al. (2011). Anti-Smo (Santa Cruz Biotechnology), anti-actin, and immunoreactive bands were revealed by chemiluminescent detection (Pierce) of peroxidase-conjugated, subtype-specific antibody (mouse IgG, Dianova) or LICOR.

Quantification and Statistical Analysis

Confocal laser scanning (Zeiss LSM5; Zeiss LSM710) or epifluorescence (Zeiss, Axiophot; Olympus BX61) microscopes were used to quantify immunopositive cells in sections or cell culture. For each quantification at least three animals or experimental culture batches were examined. All quantifications of immunostainings are based on analysis of at least five sections per animal, and the incidence of immunopositive cells is expressed either relative to the total cell number (5,000–7,000 DAPI-stained nuclei per section) or the number of GFP+ cells in the case of reporter mice. Data were tested for normal distribution and significance tests were chosen accordingly (two-tailed unpaired Student's t test or two-tailed Mann-Whitney test). Data were plotted as mean per section/culture ± SEM and significance was indicated as $^{*}p < 0.05$, $^{**}p < 0.01$, and $^{***}p < 0.001$. Quantitative analysis of western blots was performed by densitometry of both SHH bands (52 kDa multimers and 25 kDa monomers), and the values were pooled and expressed relative to actin normalized to the contralateral or intact cortex.

SUPPLEMENTAL INFORMATION

Supplemental Information for this article includes five figures and Supplemental Experimental Procedures and can be found with this article online at http://dx.doi.org/10.1016/j.stem.2013.01.019.

ACKNOWLEDGMENTS

We are particularly grateful to Andreas Faissner for providing the 473HD antibody and would like to thank Gabi Jäger, Angelika Waiser, Ines Mühlhahn, Andrea Steiner, Tatjana Simon-Ebert, and Uta Mamrak for excellent technical assistance, and Timucin Öztürk and Detlef Franzen for help with the colony of Smoothened floxed mice. It is a pleasure to thank Benedikt Berninger, Marisa Karow, Jovica Ninkovic, Stefanie Robel, and Paul Hardy for excellent comments on the manuscript and the Graduate School of Systemic Neurosciences for support. Funding to M.G. was provided by SFB 596 (DFG Collaborative Research Center on Molecular Mechanisms of Neurodegeneration), SFB 870, the award of the Breuer Prize 2008 by the Hans and Ilse Breuer Foundation, the German Federal Ministry for Education and Research (BMBF), and DFG grants GO640/6-1, 7-1, and 8-1. S.S. was supported by a grant from the Friedrich Baur Foundation, M.C. by a Research Fellowship from the Alexander von Humboldt Foundation, and N.P. by an EU MicroFlow grant. L.-H.T. is an Investigator of the Howard Hughes Medical Institute and acknowledges support from NIH (RO1 Grant NS051874).

Received: May 16, 2012
Revised: December 10, 2012
Accepted: January 24, 2013
Published: April 4, 2013

REFERENCES

Alvarez, J.I., Dodelet-Devillers, A., Kebir, H., Ifergan, I., Fabre, P.J., Terouz, S., Sabbagh, M., Wosik, K., Bourbonnière, L., Bernard, M., et al. (2011). The Hedgehog pathway promotes blood-brain barrier integrity and CNS immune quiescence. Science *334*, 1727–1731.

Amankulor, N.M., Hambardzumyan, D., Pyonteck, S.M., Becher, O.J., Joyce, J.A., and Holland, E.C. (2009). Sonic hedgehog pathway activation is induced by acute brain injury and regulated by injury-related inflammation. J. Neurosci. *29*, 10299–10308.

Androutsellis-Theotokis, A., Leker, R.R., Soldner, F., Hoeppner, D.J., Ravin, R., Poser, S.W., Rueger, M.A., Bae, S.K., Kittappa, R., and McKay, R.D. (2006). Notch signalling regulates stem cell numbers in vitro and in vivo. Nature *442*, 823–826.

Antos, C.L., and Tanaka, E.M. (2010). Vertebrates that regenerate as models for guiding stem cells. Adv. Exp. Med. Biol. *695*, 184–214.

Bambakidis, N.C., Petrullis, M., Kui, X., Rothstein, B., Karampelas, I., Kuang, Y., Selman, W.R., LaManna, J.C., and Miller, R.H. (2012). Improvement of neurological recovery and stimulation of neural progenitor cell proliferation by intrathecal administration of Sonic hedgehog. J. Neurosurg. *116*, 1114–1120.

Barnabé-Heider, F., Göritz, C., Sabelström, H., Takebayashi, H., Pfrieger, F.W., Meletis, K., and Frisén, J. (2010). Origin of new glial cells in intact and injured adult spinal cord. Cell Stem Cell *7*, 470–482.

Baumgart, E.V., Barbosa, J.S., Bally-Cuif, L., Götz, M., and Ninkovic, J. (2012). Stab wound injury of the zebrafish telencephalon: a model for comparative analysis of reactive gliosis. Glia *60*, 343–357.

Behrendt, G., Baer, K., Buffo, A., Curtis, M.A., Faull, R.L., Rees, M.I., Götz, M., and Dimou, L. (2013). Dynamic changes in myelin aberrations and oligodendrocyte generation in chronic amyloidosis in mice and men. Glia *61*, 273–286.

Boncristiano, S., Calhoun, M.E., Howard, V., Bondolfi, L., Kaeser, S.A., Wiederhold, K.H., Staufenbiel, M., and Jucker, M. (2005). Neocortical synaptic bouton number is maintained despite robust amyloid deposition in APP23 transgenic mice. Neurobiol. Aging *26*, 607–613.

Bozoyan, L., Khlghatyan, J., and Saghatelyan, A. (2012). Astrocytes control the development of the migration-promoting vasculature scaffold in the postnatal brain via VEGF signaling. J. Neurosci. *32*, 1687–1704.

Buffo, A., Rite, I., Tripathi, P., Lepier, A., Colak, D., Horn, A.P., Mori, T., and Götz, M. (2008). Origin and progeny of reactive gliosis: A source of multipotent cells in the injured brain. Proc. Natl. Acad. Sci. USA *105*, 3581–3586.

Chen, J.K., Taipale, J., Cooper, M.K., and Beachy, P.A. (2002). Inhibition of Hedgehog signaling by direct binding of cyclopamine to Smoothened. Genes Dev. *16*, 2743–2748.

Cruz, J.C., Tseng, H.C., Goldman, J.A., Shih, H., and Tsai, L.H. (2003). Aberrant Cdk5 activation by p25 triggers pathological events leading to neurodegeneration and neurofibrillary tangles. Neuron *40*, 471–483.

Cruz, J.C., Kim, D., Moy, L.Y., Dobbin, M.M., Sun, X., Bronson, R.T., and Tsai, L.H. (2006). p25/cyclin-dependent kinase 5 induces production and intraneuronal accumulation of amyloid beta in vivo. J. Neurosci. *26*, 10536–10541.

De Strooper, B., Annaert, W., Cupers, P., Saftig, P., Craessaerts, K., Mumm, J.S., Schroeter, E.H., Schrijvers, V., Wolfe, M.S., Ray, W.J., et al. (1999). A presenilin-1-dependent gamma-secretase-like protease mediates release of Notch intracellular domain. Nature *398*, 518–522.

Denes, A., Vidyasagar, R., Feng, J., Narvainen, J., McColl, B.W., Kauppinen, R.A., and Allan, S.M. (2007). Proliferating resident microglia after focal cerebral ischaemia in mice. J. Cereb. Blood Flow Metab. *27*, 1941–1953.

Duyckaerts, C., Delatour, B., and Potier, M.C. (2009). Classification and basic pathology of Alzheimer disease. Acta Neuropathol. *118*, 5–36.

El-Zaatari, M., Daignault, S., Tessier, A., Kelsey, G., Travnikar, L.A., Cantu, E.F., Lee, J., Plonka, C.M., Simeone, D.M., Anderson, M.A., and Merchant, J.L. (2012). Plasma Shh levels reduced in pancreatic cancer patients. Pancreas *41*, 1019–1028.

Fitch, M.T., and Silver, J. (2008). CNS injury, glial scars, and inflammation: Inhibitory extracellular matrices and regeneration failure. Exp. Neurol. *209*, 294–301.

Frank-Kamenetsky, M., Zhang, X.M., Bottega, S., Guicherit, O., Wichterle, H., Dudek, H., Bumcrot, D., Wang, F.Y., Jones, S., Shulok, J., et al. (2002). Small-molecule modulators of Hedgehog signaling: identification and characterization of Smoothened agonists and antagonists. J. Biol. *1*, 10.

Gabay, L., Lowell, S., Rubin, L.L., and Anderson, D.J. (2003). Deregulation of dorsoventral patterning by FGF confers trilineage differentiation capacity on CNS stem cells in vitro. Neuron *40*, 485–499.

Gadea, A., Schinelli, S., and Gallo, V. (2008). Endothelin-1 regulates astrocyte proliferation and reactive gliosis via a JNK/c-Jun signaling pathway. J. Neurosci. *28*, 2394–2408.

Garcia, A.D., Petrova, R., Eng, L., and Joyner, A.L. (2010). Sonic hedgehog regulates discrete populations of astrocytes in the adult mouse forebrain. J. Neurosci. *30*, 13597–13608.

Gates, M.A., Thomas, L.B., Howard, E.M., Laywell, E.D., Sajin, B., Faissner, A., Götz, B., Silver, J., and Steindler, D.A. (1995). Cell and molecular analysis of the developing and adult mouse subventricular zone of the cerebral hemispheres. J. Comp. Neurol. *361*, 249–266.

Göritz, C., Dias, D.O., Tomilin, N., Barbacid, M., Shupliakov, O., and Frisén, J. (2011). A pericyte origin of spinal cord scar tissue. Science *333*, 238–242.

Hashimoto, M., Ishii, K., Nakamura, Y., Watabe, K., Kohsaka, S., and Akazawa, C. (2008). Neuroprotective effect of sonic hedgehog up-regulated in Schwann cells following sciatic nerve injury. J. Neurochem. *107*, 918–927.

Huang, X., Ketova, T., Fleming, J.T., Wang, H., Dey, S.K., Litingtung, Y., and Chiang, C. (2009). Sonic hedgehog signaling regulates a novel epithelial progenitor domain of the hindbrain choroid plexus. Development *136*, 2535–2543.

Kamphuis, W., Orre, M., Kooijman, L., Dahmen, M., and Hol, E.M. (2012). Differential cell proliferation in the cortex of the APPswePS1dE9 Alzheimer's disease mouse model. Glia *60*, 615–629.

Kroehne, V., Freudenreich, D., Hans, S., Kaslin, J., and Brand, M. (2011). Regeneration of the adult zebrafish brain from neurogenic radial glia-type progenitors. Development *138*, 4831–4841.

Lai, K., Kaspar, B.K., Gage, F.H., and Schaffer, D.V. (2003). Sonic hedgehog regulates adult neural progenitor proliferation in vitro and in vivo. Nat. Neurosci. *6*, 21–27.

Lang, B., Liu, H.L., Liu, R., Feng, G.D., Jiao, X.Y., and Ju, G. (2004). Astrocytes in injured adult rat spinal cord may acquire the potential of neural stem cells. Neuroscience *128*, 775–783.

Long, F., Zhang, X.M., Karp, S., Yang, Y., and McMahon, A.P. (2001). Genetic manipulation of hedgehog signaling in the endochondral skeleton reveals a direct role in the regulation of chondrocyte proliferation. Development *128*, 5099–5108.

Machold, R., Hayashi, S., Rutlin, M., Muzumdar, M.D., Nery, S., Corbin, J.G., Gritli-Linde, A., Dellovade, T., Porter, J.A., Rubin, L.L., et al. (2003). Sonic hedgehog is required for progenitor cell maintenance in telencephalic stem cell niches. Neuron *39*, 937–950.

März, M., Schmidt, R., Rastegar, S., and Strähle, U. (2011). Regenerative response following stab injury in the adult zebrafish telencephalon. Dev. Dyn. *240*, 2221–2231.

Mori, T., Tanaka, K., Buffo, A., Wurst, W., Kühn, R., and Götz, M. (2006). Inducible gene deletion in astroglia and radial glia—a valuable tool for functional and lineage analysis. Glia *54*, 21–34.

Nakamura, T., Colbert, M.C., and Robbins, J. (2006). Neural crest cells retain multipotential characteristics in the developing valves and label the cardiac conduction system. Circ. Res. *98*, 1547–1554.

Ohlig, S., Farshi, P., Pickhinke, U., van den Boom, J., Höing, S., Jakuschev, S., Hoffmann, D., Dreier, R., Schöler, H.R., Dierker, T., et al. (2011). Sonic hedgehog shedding results in functional activation of the solubilized protein. Dev. Cell *20*, 764–774.

Plesnila, N., Zhu, C., Culmsee, C., Gröger, M., Moskowitz, M.A., and Blomgren, K. (2004). Nuclear translocation of apoptosis-inducing factor after focal cerebral ischemia. J. Cereb. Blood Flow Metab. *24*, 458–466.

Radde, R., Bolmont, T., Kaeser, S.A., Coomaraswamy, J., Lindau, D., Stoltze, L., Calhoun, M.E., Jäggi, F., Wolburg, H., Gengler, S., et al. (2006). Abeta42-driven cerebral amyloidosis in transgenic mice reveals early and robust pathology. EMBO Rep. *7*, 940–946.

Robel, S., Berninger, B., and Götz, M. (2011a). The stem cell potential of glia: lessons from reactive gliosis. Nat. Rev. Neurosci. *12*, 88–104.

Robel, S., Bardehle, S., Lepier, A., Brakebusch, C., and Götz, M. (2011b). Genetic deletion of cdc42 reveals a crucial role for astrocyte recruitment to the injury site in vitro and in vivo. J. Neurosci. *30*, 12471–12482.

Rodríguez, J.J., Olabarria, M., Chvatal, A., and Verkhratsky, A. (2009). Astroglia in dementia and Alzheimer's disease. Cell Death Differ. *16*, 378–385.

Rupp, N.J., Wegenast-Braun, B.M., Radde, R., Calhoun, M.E., and Jucker, M. (2011). Early onset amyloid lesions lead to severe neuritic abnormalities and local, but not global neuron loss in APPPS1 transgenic mice. Neurobiol. Aging *32*, 2324.e1-6.

Sehgal, R., Sheibani, N., Rhodes, S.J., and Belecky Adams, T.L. (2009). BMP7 and SHH regulate Pax2 in mouse retinal astrocytes by relieving TLX repression. Dev. Biol. *332*, 429–443.

Shimada, I.S., LeComte, M.D., Granger, J.C., Quinlan, N.J., and Spees, J.L. (2012). Self-renewal and differentiation of reactive astrocyte-derived neural stem/progenitor cells isolated from the cortical peri-infarct area after stroke. J. Neurosci. *32*, 7926–7940.

Simon, C., Götz, M., and Dimou, L. (2011). Progenitors in the adult cerebral cortex: cell cycle properties and regulation by physiological stimuli and injury. Glia *59*, 869–881.

Sims, J.R., Lee, S.W., Topalkara, K., Qiu, J., Xu, J., Zhou, Z., and Moskowitz, M.A. (2009). Sonic hedgehog regulates ischemia/hypoxia-induced neural progenitor proliferation. Stroke *40*, 3618–3626.

Sirko, S., Neitz, A., Mittmann, T., Horvat-Bröcker, A., von Holst, A., Eysel, U.T., and Faissner, A. (2009). Focal laser-lesions activate an endogenous population of neural stem/progenitor cells in the adult visual cortex. Brain *132*, 2252–2264.

Sofroniew, M.V. (2009). Molecular dissection of reactive astrogliosis and glial scar formation. Trends Neurosci. *32*, 638–647.

Stoick-Cooper, C.L., Moon, R.T., and Weidinger, G. (2007). Advances in signaling in vertebrate regeneration as a prelude to regenerative medicine. Genes Dev. *21*, 1292–1315.

Sturchler-Pierrat, C., Abramowski, D., Duke, M., Wiederhold, K.H., Mistl, C., Rothacher, S., Ledermann, B., Bürki, K., Frey, P., Paganetti, P.A., et al. (1997). Two amyloid precursor protein transgenic mouse models with Alzheimer disease-like pathology. Proc. Natl. Acad. Sci. USA *94*, 13287–13292.

Traiffort, E., Charytoniuk, D., Watroba, L., Faure, H., Sales, N., and Ruat, M. (1999). Discrete localizations of hedgehog signalling components in the developing and adult rat nervous system. Eur. J. Neurosci. *11*, 3199–3214.

Tsuda, M., Kohro, Y., Yano, T., Tsujikawa, T., Kitano, J., Tozaki-Saitoh, H., Koyanagi, S., Ohdo, S., Ji, R.R., Salter, M.W., and Inoue, K. (2011). JAK-STAT3 pathway regulates spinal astrocyte proliferation and neuropathic pain maintenance in rats. Brain *134*, 1127–1139.

Veeraraghavalu, K., Choi, S.H., Zhang, X., and Sisodia, S.S. (2010). Presenilin 1 mutants impair the self-renewal and differentiation of adult murine subventricular zone-neuronal progenitors via cell-autonomous mechanisms involving notch signaling. J. Neurosci. *30*, 6903–6915.